PROCEEDINGS OF SCIENCE

Searches for BSM physics using challenging and long-lived signatures with the ATLAS detector

Xiangxuan Zheng[a,*] **on behalf of the ATLAS collaboration**

[a] *State Key Laboratory of Particle Detection and Electronics, University of Science and Technology of China, Hefei 230026, China*

E-mail: zxx0209@mail.ustc.edu.cn

Many Beyond the Standard Model (BSM) theories predict the existence of long-lived particles (LLPs), which can exhibit unusual experimental signatures. Standard reconstruction algorithms may inadvertently miss events or objects containing LLPs, making dedicated searches essential to uncover these signals. This presentation will discuss recent results from LLP searches using the ATLAS detector.

The 43rd International Symposium on Physics in Collision,
22-25 October 2024
National Centre for Scientific Research "Demokritos", Athens, Greece

*Speaker

© Copyright owned by the author(s) under the terms of the Creative Commons Attribution-NonCommercial-NoDerivatives 4.0 International License (CC BY-NC-ND 4.0) All rights for text and data mining, AI training, and similar technologies for commercial purposes, are reserved. ISSN 1824-8039 . Published by SISSA Medialab.

PoS(PIC2024)042

1. Overview

The discovery of the Higgs boson in 2012 marked the completion of the Standard Model. However, several unresolved issues, such as dark matter, matter-antimatter asymmetry of the universe, and the nature of gravity, remain beyond its scope. Various BSM theories have been proposed to address these challenges. Many of these theories predict new particles with suppressed decays due to weak coupling constants, limited decay phase space due to compact mass spectra, or heavy mediators, resulting in long lifetimes and classifying them as LLPs. Recent searches for LLPs at the ATLAS experiment [1] aim to detect these signals across various BSM scenarios.

1. **Hidden Sector(HS) Model [2, 3]**: The HS model addresses the hierarchy problem by connecting the SM and HS through a heavy neutral scalar boson (Φ), which decays into two long-lived neutral scalar bosons (s). The Φ, potentially the SM Higgs boson, may be produced with a vector boson (W/Z) or via vector boson fusion (VBF). The s bosons subsequently decay into quarks or gluons.

2. **Axion-like Particle(ALP) models [4–6]**: ALPs, which may resolve the strong CP problem, are predicted to have long lifetimes in specific parameter spaces. The Higgs boson can decay into two ALPs, with each ALP decaying into two photons. Additionally, the ALP a can couple to gluons and W/Z bosons through dimension-5 operators, though with a suppressed photon coupling. This interaction results in the production of a alongside a vector boson, which then decays into gluons. The ALP can also couple to up-type quarks, leading to exotic top quark decays ($t \to ac/au$) in $t\bar{t}$ events, primarily decaying into charm quark pairs or gluons, depending on its mass m_a.

3. HZZ_d **model [7]**: This model predicts a hadronically decaying, long-lived neutral particle, Z_d, produced with a SM Z boson through a scalar mediator connecting SM and HS, represented by $pp \to \Phi \to ZZ_d$, where $Z \to \ell^+\ell^-(\ell = e, \mu)$. The Z_d may be seen as a dark photon, while Φ is the SM Higgs boson.

4. **Falkowski Ruderman-Volansky-Zupan (FRVZ) model [8]**: This model predicts the production of a long-lived dark photon (γ_d), mediating a broken dark U(1) gauge interaction within the dark sector and kinetically mixing with the SM hypercharge. A pair of dark fermions f_d is produced through Higgs decay, with each f_d decaying into a dark photon and a stable dark fermion, assumed as the undetected hidden lightest stable particle (HLSP). This results in final states with two dark photons decaying into SM fermions.

5. **Gauge-Mediated Supersymmetry Breaking (GMSB) model [9]**: In this model, the lightest SUSY particle (LSP) is a nearly massless gravitino ($\tilde{G}$). The next-to-lightest SUSY particle (NLSP) is a long-lived slepton ($\tilde{\ell}$), which can be a selectron ($\tilde{e}$), smuon ($\tilde{\mu}$), or stau ($\tilde{\tau}$).

The experimental signatures of LLPs at the LHC are diverse and often differ significantly from standard SM processes. Standard reconstruction algorithms may miss events or objects containing LLPs due to their unusual characteristics. Consequently, dedicated searches are essential to detect LLP signals.

PoS(PIC2024)042

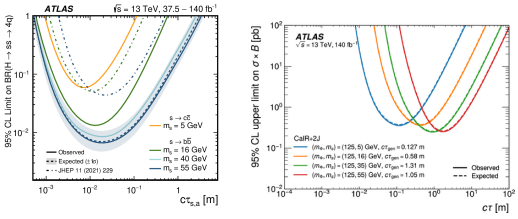

(a) (b)

Figure 1: Observed (solid line) and expected (dashed line) upper limits at the 95% CL on the cross-section times branching fraction as a function of $c\tau$ for s decay in (a) ID [10] and (b) HCal [11].

This proceeding will introduce five recent searches for LLPs at the ATLAS detector, categorized by different types of LLPs.

2. Searches for LLP

2.1 Search for Long-lived Neutral Scalar Bosons

Neutral scalar bosons s in the HS model can decay hadronically, producing displaced jets in the inner detector (ID) and the hadronic calorimeter (HCal). Two analyses focus on these decays.

An analysis investigates the decay of s in the ID [10]. These decays produce a unique signature characterized by one or more hadronic jets originating from a significantly displaced position relative to the pp collision point, known as a displaced vertex (DV). The main background consists of SM hadronic jets. Jets from the decay products of s, termed *displaced jets*, have a distinct topology compared to *prompt jets* originating from a pp interaction vertex. A per-jet boosted decision tree (BDT) is trained to differentiate displaced jets from prompt jets. A higher BDT score indicates a greater likelihood of the jet originating from a displaced decay. All events considered in the analysis must have at least two jets with a BDT score above 0.5. Signal regions (SRs) are defined by the event-level discriminant ($BDT_{j_0} \times BDT_{j_1}$, derived from the two jets with the highest BDT scores) and the number of DVs. A data-driven method is used to estimate the background.

Another analysis examines the decays of s in the HCal [11]. For jets from s that decay after passing through the electromagnetic calorimeter (ECal), the ratio of energy in the hadronic calorimeter to that in the ECal, known as CalRatio, can be significantly higher than that of non-prompt SM jets and other backgrounds. Jets with these characteristics are termed CalRatio jets. The primary background includes SM hadronic jets and non-collision backgrounds (NCBs) such as beam-induced background (BIB) and cosmic rays. A neural network (NN) is trained to distinguish signal-like jets from BIB-like jets and SM multi-jets. An event-level NN is used to eliminate all BIB events during selection. The final background estimate is data-driven, utilizing the likelihood-based ABCD method described in Ref [12].

Both analyses use 140 fb^{-1} of pp collision data at $\sqrt{s}$ = 13 TeV, collected by the ATLAS detector from 2015 to 2018. No significant excess beyond the SM prediction is observed, and the upper limits at 95% confidence level (CL) have been improved with respect to previous results, as shown in Figure 1.

PoS(PIC2024)042

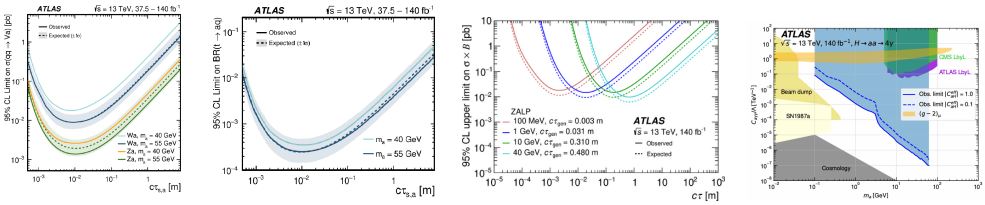

(a) (b) (c) (d)

Figure 2: Upper limits at 95% CL for ALPs with signatures of (a) (b) displaced jets [10], (c) CalRatio jets [11], and (d) photon showers [13].

2.2 Search for Long-lived ALPs

Three analyses are conducted on ALPs across different production modes.

The first analysis investigates ALPs produced through vector boson interactions or from exotic top quark decays in the ID [10]. These ALPs can decay hadronically, resulting in displaced jets. These jets exhibit signatures similar to those described in the first analysis of Section 2.1.

The second analysis focuses on ALPs produced through vector boson interactions that decay hadronically in the HCal [11], producing CalRatio jets as described in the second analysis of Section 2.1. The primary backgrounds include SM processes involving vector bosons with jets, and single or pair production of top quarks. The same NN is trained to distinguish signal-like jets from BIB-like and SM multi-jets, while BDTs are trained using different input signal samples to identify signal events from background events.

The third analysis examines ALPs in the process $H \to aa \to 4\gamma$, involving the reconstruction of photons from topologically connected clusters of energy deposits in the ECal [13]. Standard photon identification criteria are applied in final states where individual photons can be reconstructed separately. ALPs with small masses predominantly decay into a pair of highly collimated photons, reconstructed as a single photon object. Consequently, two NNs are trained to identify the signal events. The first network distinguishes real photon signatures, whether single or collimated, from the multi-jet background. The second network separates single-photon from collimated signatures. A data-driven sideband method is employed to estimate the background.

All analyses use 140 fb^{-1} of pp collision data at $\sqrt{s}$ = 13 TeV collected by the ATLAS detector from 2015 to 2018. No significant excess beyond the SM prediction is observed. For the hadronically decaying long-lived ALPs, upper limits at 95% CL have been set for the first time in certain parameter spaces. For ALPs decaying into photons, upper limits have been improved in specific parameter spaces, as shown in Figure 2.

2.3 Search for Light Long-lived Dark Photons

Dark photons are predicted to decay into SM fermions, leading to displaced jets in the calorimeter or muon spectrometer (MS). Two analyses focus on dark photons.

The first analysis considers the HZZ_d model [11]. The decay products of dark photons generate CalRatio jets in the HCal, analyzed using the same strategy as described in the second analysis of Section 2.2.

PoS(PIC2024)042

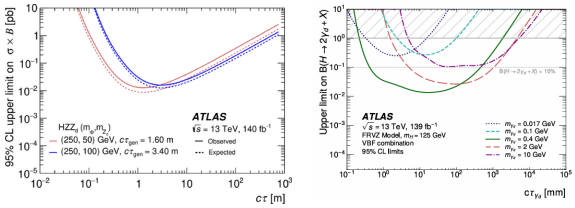

(a) (b)

Figure 3: 95% CL upper limits on (a) $\sigma \times B$ versus $c\tau$ in the HZZ_d model [11], and (b) B versus $c\tau_{\gamma_d}$ in the FRVZ model [14], where $c\tau$ and $c\tau_{\gamma_d}$ are the mean proper decay lengths of the dark photon in each model.

The second analysis examines the FRVZ model [14]. Decay products of dark photons are expected to form dark-photon jets (DPJs) akin to conventional jets. The primary backgrounds are QCD hadronic jets and non-collision backgrounds (NCBs). Displaced DPJs, reconstructed in the calorimeter or MS, are analyzed. A dark photon decaying into muons outside the ID is expected to produce two or more collimated standalone MS tracks, termed muonic dark-photon jets (μDPJs). A dense neural network (DNN) is trained to identify signal μDPJs and reject those originating from cosmic-ray backgrounds. Dark photons decaying into electron or quark pairs in the HCal with a high CalRatio are referred to as calorimeter dark-photon-jet candidates (caloDPJs). A convolutional neural network (CNN) is trained to distinguish caloDPJs from QCD prompt jets. The ABCD method is used for data-driven background estimation. This analysis utilizes 139 fb^{-1} of pp collision data at $\sqrt{s}$ = 13 TeV collected by the ATLAS detector from 2015 to 2018.

For both analyses, no significant excess beyond the SM prediction is observed. The upper limits at 95% CL have been improved for various models, as shown in Figure 3.

2.4 Search for Long-Lived Sleptons

In the GMSB model, each pair-produced slepton can decay into a charged SM lepton (ℓ) of the same flavor and a gravitino LSP, resulting in events that contain two displaced leptons. The primary backgrounds include fake and heavy-flavor (FHF) leptons and cosmic ray muons. The analysis focuses on a search for sleptons.

This is the first LLP search utilizing LHC Run 3 data [15]. Compared to the previous Run 2 ATLAS displaced lepton search, this analysis employs new large radius tracking (LRT) to reconstruct displaced tracks. LRT has been improved to reduce the number of incorrectly reconstructed tracks and decrease computation time, enabling LRT tracks to be reconstructed in all events. The Liquid Argon (LAr) calorimeter has been implemented to provide high-precision timing, achieving a timing resolution of approximately 200 ps. Since displaced electrons can be reconstructed as photons, two BDTs are trained to distinguish displaced electrons from particles reconstructed as either electrons or photons, known as EM-BDT analysis. The ABCD method and EM-BDT are utilized independently for data-driven background estimation.

The analysis uses 56.3 fb^{-1} of pp collision data at $\sqrt{s}$ = 13.6 TeV collected during 2022-2023 and 140 fb^{-1} of data at $\sqrt{s}$ = 13 TeV collected during 2015-2018. No significant excess beyond the SM prediction is observed. Incorporating early Run 3 data along with new triggers has improved sensitivity compared to prior searches, as shown in Figure 4.

PoS(PIC2024)042

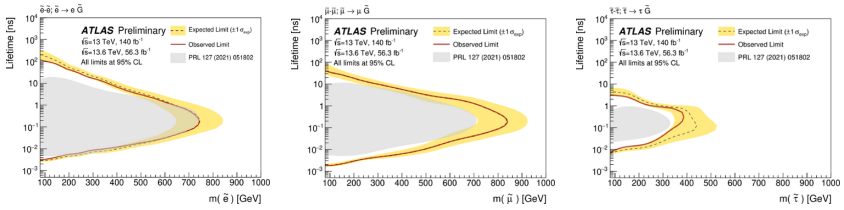

(a) (b) (c)

Figure 4: Expected and observed 95% CL exclusion contours for the (a) selectron, (b) smuon, and (c) stau models.[15]

3. Summary

Within ATLAS, numerous searches for LLPs focus on exploring BSM physics. Detecting LLP signals presents a significant challenge, as conventional search methods might inadvertently exclude LLPs. To date, no significant excess beyond the SM prediction has been observed. However, search sensitivity continues to improve with advancements in algorithms and detector technology. More exciting results are anticipated from the Run 3 data in the future.

References

[1] ATLAS Collaboration, JINST 3 (2008) S08003.

[2] M. J. Strassler and K. M. Zurek, Phys. Lett. B 661 (2008) 263, arXiv: hep-ph/0605193.

[3] S. Chang et al., Ann. Rev. Nucl. Part. Sci. 58 (2008) 75, arXiv: 0801.4554.

[4] I. Brivio et al., Eur. Phys. J. C 77 (2017) 572, arXiv: 1701.05379.

[5] A. Carmona et al., JHEP 07 (2022) 122, arXiv: 2202.09371.

[6] M. Bauer et al., JHEP 12 (2017) 044, arXiv: 1708.00443.

[7] H. Davoudiasl et al., Phys. Rev. D 88 (2013) 015022, arXiv: 1304.4935.

[8] A. Falkowski et al., Phys. Rev. Lett. 105 (2010) 241801, arXiv: 1007.3496.

[9] D. Alves et al., J. Phys. G 39 (2012) 105005, arXiv: 1105.2838.

[10] ATLAS Collaboration, PRL 133 (2024) 161803, arXiv: 2403.15332.

[11] ATLAS Collaboration, JHEP 11 (2024) 036, arXiv: 2407.09183.

[12] ATLAS Collaboration, JHEP 06 (2022) 005, arXiv: 2203.01009.

[13] ATLAS Collaboration, Eur. Phys. J. C 84 (2024) 742, arXiv: 2312.03306.

[14] ATLAS Collaboration, Eur. Phys. J. C 84 (2024) 719, arXiv: 2311.18298.

[15] ATLAS Collaboration. arXiv: 2410.16835.

PoS(PIC2024)042